Accurate and Fast Extraction of the Bloch Eigenmodes of Fiber Gratings

Amir M. Jazayeri[*]

Abstract—Based on Bloch-Floquet's theorem and ordinary matrix calculations, a rigorous method for extraction of the eigenmodes of fiber gratings is developed. This method is also applicable to fiber gratings which are either physically multilayer or mathematically divided into layers along the radial coordinate. Although the well-known coupled mode theory (CMT) is accounted a method for extraction of the coefficients of reflection and transmission of finite-length FBGs, its inadequacy for extraction of the Bloch eigenmodes of FBGs is illustrated, even if the modulation depth of refractive index is small and the Bragg condition is satisfied.

1. INTRODUCTION

For a waveguide grating, which is periodic along the longitudinal coordinate z, Bloch-Floquet's theorem states that the electromagnetic fields everywhere are quasi-periodic functions of z, and can be written as quasi-Fourier series versus z, i.e., Fourier series versus z multiplied by a common factor consisting of the Bloch wavenumber [1]. This is in contrast to the viewpoint of some authors who introduce an artificial periodicity in the transverse direction [2, 3], or who do not use the physical/artificial periodicity [4, 5].

The cylindrical coordinates (r, φ, z) are naturally used for a fiber grating, which is periodic along the z-axis. The rigorous method proposed in Section 2 resembles Fourier modal methods for planar diffraction gratings [6, 7], although the Bloch wavenumber is predetermined by the incident plane wave for diffraction problems, and is to be found here.

Unlike the analysis of fiber gratings presented in [1], instead of numerically solving *four coupled differential* equations for the four components E_z, H_z, E_φ, and H_φ, *two uncoupled matrix* eigenproblems for the first two components are derived in Section 2, then the other two components are derived accordingly. The proposed rigorous method can be used for a multilayer fiber grating, i.e., a fiber grating with concentric shells [8, 9]. It is also applicable to other types of fiber gratings by dividing the structure into large enough number of layers along the radial coordinate.

Traditionally, analysis of a fiber Bragg gratings (FBG), which by definition has small modulation depth of refractive index along the z-axis, is performed via coupled mode theory (CMT) [10–13]. According to the literature, CMT is a method for extraction of the coefficients of reflection and transmission of a finite-length FBG inscribed into an ordinary optical fiber. However, the fact that the Bloch eigenmodes of an FBG can also be extracted by CMT is often overlooked [14], and therefore, is emphasized in Section 3. However small modulation depth of refractive index is chosen, and even if the Bragg condition is satisfied, striking discrepancy between the Bloch wavenumbers extracted by CMT and by the proposed rigorous method is illustrated in Section 4.

2. PROPOSED RIGOROUS METHOD

A simple FBG consists of a longitudinally periodic core which is placed in an homogeneous environment with a relative permittivity ε_s, but the rigorous method to be proposed here is also applicable to fiber

* Corresponding author: Amir M. Jazayeri (amirjazaayeri@gmail.com).
The author is with the Department of Electrical Engineering, Sharif University of Technology, Tehran 145888-9694, Iran.
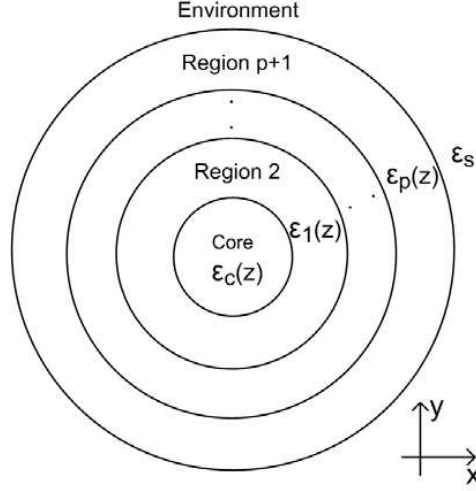
Figure 1. The generic structure which the proposed method is applicable to. The environment is a homogeneous material. The other *regions* are each either homogenous or periodic along the z-axis with a common period.

gratings which have p layers between the core and the environment as depicted in Fig. 1. These layers can have different longitudinally periodic permittivities but with the same period Λ as the core.

Each of the Bloch eigenmodes of this fiber has an azimuthal variation $e^{jm\varphi}$, where $m = 0, 1, 2, \ldots$. It is worth noting that the TE ($E_z = 0$) and TM ($H_z = 0$) Bloch eigenmodes exist only when $m = 0$.

The relative permittivity and its inverse in each *region*, including the environment as a homogenous material, can be written as Fourier series versus z as follows:

$$\varepsilon_r(z) = \sum_l \varepsilon_{r_l} e^{jl\frac{2\pi}{\Lambda}z}, \tag{1}$$

$$\frac{1}{\varepsilon_r(z)} = \sum_l \eta_{r_l} e^{jl\frac{2\pi}{\Lambda}z}, \tag{2}$$

where $\varepsilon_r(z)$ is the relative permittivity of that *region*. Based on Bloch-Floquet's theorem, the electromagnetic fields in that *region* can also be written as quasi-Fourier series versus z, i.e., Fourier series versus z multiplied by a common factor $e^{j\kappa z}$, where κ is the Bloch wavenumber which has to be found. Therefore, the quasi-Fourier series for E_z, H_z, E_φ, and H_φ in each *region* read as

$$E_z = e^{jm\varphi}e^{j\kappa z}\sum_l e^{jl\frac{2\pi}{\Lambda}z}e_{z_l}(r), \tag{3}$$

$$H_z = e^{jm\varphi}e^{j\kappa z}\sum_l e^{jl\frac{2\pi}{\Lambda}z}h_{z_l}(r), \tag{4}$$

$$E_\varphi = e^{jm\varphi}e^{j\kappa z}\sum_l e^{jl\frac{2\pi}{\Lambda}z}e_{\varphi_l}(r), \tag{5}$$

$$H_\varphi = e^{jm\varphi}e^{j\kappa z}\sum_l e^{jl\frac{2\pi}{\Lambda}z}h_{\varphi_l}(r), \tag{6}$$

where $\{e_{z_l}(r)\}$, $\{h_{z_l}(r)\}$, $\{e_{\varphi_l}(r)\}$, and $\{h_{\varphi_l}(r)\}$ are four sets of unknown r-dependent coefficients peculiar to that *region*. In practice, all the Fourier/quasi-Fourier series have to be truncated up to N harmonics in total: $-M \le l \le M$ if $N = 2M + 1$, and $-M \le l \le M - 1$ if $N = 2M$.

Unlike Ref. [1], instead of numerically solving *four coupled differential* equations for the four components E_z, H_z, E_φ, and H_φ, we begin with E_z and H_z for which *two uncoupled matrix*

eigenproblems are derived. As discussed in Appendix, the equations

$$k_0^2 \varepsilon_r E_z + \frac{\partial}{\partial z}\left(\frac{1}{\varepsilon_r}\frac{\partial}{\partial z}(\varepsilon_r E_z)\right) = -\nabla_t^2 E_z, \tag{7}$$

$$k_0^2 \varepsilon_r H_z + \frac{\partial}{\partial z^2}H_z = -\nabla_t^2 H_z, \tag{8}$$

are valid within each *region*, where $\varepsilon_r(z)$ is the relative permittivity of the *region*, $e^{j\omega t}$ is the time variation, $k_0 = \omega\sqrt{\mu_0\varepsilon_0}$, and $\nabla_t^2 = \nabla^2 - \frac{\partial^2}{\partial z^2}$. By introducing the right-hand sides of Eqs. (1), (2), and (3) into Eq. (7), and taking into consideration the linear independence of the functions $\{e^{jl\frac{2\pi}{\Lambda}z}\}$ from each other on $0 < z < \Lambda$, the following relationship is obtained in each *region*:

$$\left(k_0^2[[\varepsilon_r]] - K[[1/\varepsilon_r]]K[[\varepsilon_r]]\right)[E_z] = -\left(\frac{\partial^2}{\partial r^2} + \frac{1}{r}\frac{\partial}{\partial r} - \frac{m^2}{r^2}\right)[E_z], \tag{9}$$

where $[E_z]$ denotes a column vector consisting of the functions $\{e_{z_l}(r)\}$ in that *region*, K a diagonal matrix with the diagonal entries $\kappa + l2\pi/\Lambda$, and $[[f]]$ a Toeplitz matrix whose entry $[[f]]_{pq}$ is the coefficient $p - q$ in the Fourier series of $f(z)$. Therefore, the general solution to Eq. (9) is in the form of

$$[E_z] = \sum_n \left(a_n^e H_m^{(2)}(k_n^e r) + b_n^e H_m^{(1)}(k_n^e r)\right)\vec{V}_n^e, \tag{10}$$

where $\{a_n^e\}$ and $\{b_n^e\}$ are two sets of unknown coefficients peculiar to that *region*, and $k_n^{e^2}$ and $\vec{V}_n^e$ are the nth eigenvalue and the nth eigenvector of the matrix $k_0^2[[\varepsilon_r]] - K[[1/\varepsilon_r]]K[[\varepsilon_r]]$, respectively. Similarly, Eq. (8) together with Eqs. (1) and (4) yield the following general solution to $[H_z]$ in that *region*:

$$[H_z] = \sum_n \left(a_n^h H_m^{(2)}(k_n^h r) + b_n^h H_m^{(1)}(k_n^h r)\right)\vec{V}_n^h, \tag{11}$$

where $[H_z]$ denotes a column vector consisting of the functions $\{h_{z_l}(r)\}$ in that *region*. $\{a_n^h\}$ and $\{b_n^h\}$ are two other sets of unknown coefficients peculiar to that *region*, and $k_n^{h^2}$ and $\vec{V}_n^h$ are the nth eigenvalue and the nth eigenvector of the matrix $[[\varepsilon_r]]k_0^2 - K^2$, respectively.

For the environment, which is the external *region*, only the Hankel functions $H_m^{(2)}(k_n r)$ can be retained, where

$$k_n^2 = k_n^{e^2} = k_n^{h^2} = k_0^2\varepsilon_s - \left(\kappa + n\frac{2\pi}{\Lambda}\right)^2, \tag{12}$$

and the square root of k_n^2 is defined by a criterion to be addressed at the end of this section. For the core, which includes the z-axis, the Bessel functions $J_m(k_n^e r)$ and $J_m(k_n^h r)$ should be used, i.e.,

$$[E_z] = \sum_n a_n^e J_m(k_n^e r)\vec{V}_n^e, \tag{13}$$

$$[H_z] = \sum_n a_n^h J_m(k_n^h r)\vec{V}_n^h. \tag{14}$$

In other words, for each of the environment and the core, $\{b_n^e\}$ and $\{b_n^h\}$ are zero.

The components E_φ and H_φ have yet to be found. Assuming $\mu_r = 1$, Eq. (A6) for $\vec{H}_t$ and its counterpart for $\vec{E}_t$ yield the following equations in each *region*:

$$\left[\frac{\partial}{\partial z}\left(\frac{1}{\varepsilon_r}\frac{\partial}{\partial z}\right) + k_0^2\right]H_\varphi = -j\omega\varepsilon_0\frac{\partial}{\partial r}E_z + \frac{jm}{r}\frac{\partial}{\partial z}\left(\frac{H_z}{\varepsilon_r}\right), \tag{15}$$

$$\left[\frac{\partial^2}{\partial z^2} + k_0^2\varepsilon_r\right]E_\varphi = \frac{jm}{r}\frac{\partial}{\partial z}E_z + j\omega\mu_0\frac{\partial}{\partial r}H_z. \tag{16}$$

By introducing the right-hand sides of Eqs. (2), (3), (4), and (6) into Eq. (15), and taking into consideration the linear independence of the functions $\{e^{jl\frac{2\pi}{\Lambda}z}\}$ from each other on $0 < z < \Lambda$, the following relationship is obtained in that *region*:

$$\left(-K[[1/\varepsilon_r]]K + k_0^2 I_d\right)[H_\varphi] = -j\omega\varepsilon_0\frac{\partial}{\partial r}[E_z] - \frac{m}{r}K[[1/\varepsilon_r]][H_z], \tag{17}$$

where the column vector $[H_\varphi]$ consists of the functions $\{h_{\varphi_l}(r)\}$ in that *region*, and I_d is the identity matrix. In view of Eq. (17) together with Eqs. (10) and (11), the general solution to $[H_\varphi]$ can be written in terms of the same coefficients $\{a_n^e, b_n^e, a_n^h, b_n^h\}$ used for $[E_z]$ and $[H_z]$ in that *region* according to the following relationship:

$$\left(-K[[1/\varepsilon_r]]K + k_0^2 I_d\right)[H_\varphi] = -j\omega\varepsilon_0 \sum_n \left(a_n^e H_m^{(2)'}(k_n^e r) + b_n^e H_m^{(1)'}(k_n^e r)\right)k_n^e \vec{V}_n^e$$

$$-\frac{m}{r}K[[1/\varepsilon_r]]\sum_n \left(a_n^h H_m^{(2)}\left(k_n^h r\right) + b_n^h H_m^{(1)}\left(k_n^h r\right)\right)\vec{V}_n^h, \qquad (18)$$

Similarly, Eq. (16) yields the following general solution to $[E_\varphi]$:

$$\left(-K^2 + k_0^2[[\varepsilon_r]]\right)[E_\varphi] = -\frac{m}{r}K\sum_n \left(a_n^e H_m^{(2)}(k_n^e r) + b_n^e H_m^{(1)}(k_n^e r)\right)\vec{V}_n^e$$

$$+j\omega\mu_0 \sum_n \left(a_n^h H_m^{(2)'}\left(k_n^h r\right) + b_n^h H_m^{(1)'}\left(k_n^h r\right)\right)k_n^h \vec{V}_n^h, \qquad (19)$$

where the column vector $[E_\varphi]$ consists of the functions $\{e_{\varphi_l}(r)\}$ in that *region*.

It is worth noting that the inverse multiplication rule of the Fourier factorization helps analysis of gratings whose periodic variation of refractive index has discontinuity like lamellar diffraction gratings [15]. The structures here usually have continuous variation of refractive index versus z, and therefore the formulation with Laurent's rule, which slightly differs from the formulation with the inverse multiplication rule, was proposed above. As expected, it can be seen both of the formulations render the same results for the examples given in Section 4.

From Eqs. (10), (11), (18), and (19), it is evident that an r-dependent matrix W in each *region* relates the column vector $\left([E_z]^T \quad [H_z]^T \quad [E_\varphi]^T \quad [H_\varphi]^T\right)^T$ to the column vector $\left(\vec{A}^{e^T} \quad \vec{A}^{h^T} \quad \vec{B}^{e^T} \quad \vec{B}^{h^T}\right)^T$, where the column vectors $\vec{A}^e$, $\vec{A}^h$, $\vec{B}^e$, and $\vec{B}^h$ consist of the coefficients $\{a_n^e\}$, $\{a_n^h\}$, $\{b_n^e\}$, and $\{b_n^h\}$ defined in that *region*. Therefore, by imposing boundary conditions for the column vector $\left([E_z]^T \quad [H_z]^T \quad [E_\varphi]^T \quad [H_\varphi]^T\right)^T$ at interface between two adjacent *regions*, the column vector $\left(\vec{A}^{e^T} \quad \vec{A}^{h^T} \quad \vec{B}^{e^T} \quad \vec{B}^{h^T}\right)^T$ in one side simply relates to its counterpart in the other side. By following the S-matrix algorithm as proposed in [6], a matrix equation

$$S\left(\vec{A}_c^{e^T} \quad \vec{A}_c^{h^T} \quad \vec{A}_s^{e^T} \quad \vec{A}_s^{h^T}\right)^T = \vec{0} \qquad (20)$$

is easily found, where the column vectors $\left(\vec{A}_c^{e^T} \quad \vec{A}_c^{h^T}\right)^T$ and $\left(\vec{A}_s^{e^T} \quad \vec{A}_s^{h^T}\right)^T$ belong to the core and the environment, respectively. To have a non-all-zero solution, the determinant of S has to be zero, and therefore the Bloch wavenumbers are found by locating the roots of $\det(S)$.

Generally speaking, the Bloch wavenumbers are located on the complex plane depending on the criterion whereby the square root of k_n^2 in the environment, which appeared in Eq. (12), is defined. Given the Hankel functions $H_m^{(2)}(k_n r)$ in the environment, a necessary condition for the *bounded* Bloch eigenmodes is that each k_n has a negative imaginary part so that the electromagnetic fields approach zero at $r \to \infty$. The other necessary condition for the *bounded* Bloch eigenmodes is that no power is transferred along the radial coordinate. Based on these two conditions, and by taking notice of the far-field zone with large enough r, the form of the Bloch wavenumber of a *bounded* Bloch eigenmode belongs to one of these three categories; first, $\{\kappa = \pm\kappa_R : k_0\sqrt{\varepsilon_s} < \kappa_R < \pi/\Lambda\}$, second, $\{\kappa = \pm j\kappa_I : \kappa_I > 0\}$, and third, $\{\kappa = \pi/\Lambda \pm j\kappa_I : \kappa_I > 0\}$. It is evident that $k_0\sqrt{\varepsilon_s} < \pi/\Lambda$ is a prerequisite for the existence of the first category.

As already mentioned, in practice all the Fourier/quasi-Fourier series are truncated up to N harmonics. To *numerically* make the radial transfer of power zero, the harmonics $-M \leq l \leq M - 1$ are kept ($N = 2M$) if the form of the Bloch wavenumber belongs to the third category mentioned above. Otherwise, the harmonics $-M \leq l \leq M$ are retained ($N = 2M + 1$).

3. CMT AS CONVENTIONAL METHOD

From the viewpoint based on CMT, the longitudinal periodicity of permittivity, as depicted in Fig. 1, is accounted a periodic *perturbation* in another fiber which is uniform along the z-axis, and named the *unperturbed* fiber [16]. Each of E_z, H_z, E_φ, and H_φ is written as a linear combination of the same transverse component of the modes (forward and backward) supported by the *unperturbed* fiber. Unknown coefficient of each mode in these expansions is z-dependent, and is assumed to be identical in all of the four expansions. In theory, the bounded modes and the radiation modes of the *unperturbed* fiber, whose propagation wavenumbers are discrete and continuous, respectively, have to be retained in the expansions, but in practice only the bounded modes are usually kept.

In accordance with the examples to be given in Section 4, only a simple structure consisting of a periodic core inside an environment, namely with $p = 0$ in Fig. 1, is examined here by CMT. Therefore, the associated *unperturbed* structure is a step-index fiber. If the *perturbation* in the relative permittivity of the core of the *unperturbed* fiber is $\Delta\varepsilon_r(z) = \delta\cos(2\pi z/\Lambda)$, where δ is small in comparison with the average relative permittivity of the *unperturbed* fiber, and if there is a bounded mode supported by the *unperturbed* fiber with a propagation wavenumber β_0 very close to π/Λ, this mode and its backward version (with the propagation wavenumber $-\beta_0$) have the most contribution in the CMT expansions. Therefore, the CMT equations read as:

$$dc_{\beta_0}/dz = -j\gamma e^{j2(\beta_0 - \pi/\Lambda)z}c_{-\beta_0}, \tag{21}$$

$$dc_{-\beta_0}/dz = j\gamma e^{-j2(\beta_0 - \pi/\Lambda)z}c_{\beta_0}, \tag{22}$$

where c_{β_0} and $c_{-\beta_0}$ are the z-dependent coefficients of the forward and backward modes in the CMT expansions, respectively,

$$\gamma = (\omega\varepsilon_0\delta/8)\int_{\text{core cross-section}} \vec{E}_{\beta_0}\cdot\vec{E}_{\beta_0}^* ds \tag{23}$$

is the coupling coefficient between them, and $\vec{E}_{\beta_0}$ is their normalized electric field, i.e.,

$$\int_{\infty \text{ cross-section}} \vec{E}_{\beta_0}\cdot\vec{E}_{\beta_0}^* ds = 2\omega\mu_0/\beta_0. \tag{24}$$

According to the literature, Eqs. (21) and (22) successfully yield the coefficients of reflection and transmission when the aforementioned FBG, which is inscribed into its associated *unperturbed* fiber, has a finite length L along the z-axis, and is excited by that mode of the *unperturbed* fiber with the propagation wavenumber β_0.

Apart from extraction of the coefficients of reflection and transmission, the *general* solution to the differential equations in Eqs. (21) and (22) demonstrates that the *general* solution to a transverse component of the electromagnetic fields is a linear combination of two exponential functions $e^{j\kappa z}$ and $e^{-j\kappa z}$, where $\kappa = \pi/\Lambda \pm j\sqrt{\gamma^2 - (\beta_0 - \pi/\Lambda)^2}$ is the Bloch wavenumber obtained by CMT [14]. It is worth noting that β_0, γ, and κ are all dependent on λ_0, where $\lambda_0 = 2\pi/k_0$ is the wavelength in vacuum.

4. RESULTS AND CONCLUSIONS

Discrepancy between the Bloch wavenumbers extracted by the rigorous method proposed in Section 2, and by CMT as discussed in Section 3, is illustrated. Each example is a simple FBG consisting of a periodic core with a diameter D and a relative permittivity $\Delta\varepsilon_r(z) = \varepsilon_{r_{dc}} + \delta\cos(2\pi z/\Lambda)$ inside an environment with a relative permittivity ε_s. The values $\varepsilon_{r_{dc}} = (1.4545 + 0.0022)^2$, $\delta = 2(1.4545 + 0.0022)(0.0022)$, and $\varepsilon_s = (1.45)^2$ are assumed throughout this section, which are the values used in [13]. Each FBG has an associated *unperturbed* fiber consisting of a core with the relative permittivity $\varepsilon_{r_{dc}}$ and the same diameter D inside the same environment.

For the first example, $D = 8\,\mu m$. Therefore, the associated *unperturbed* fiber is singlemode at the vacuum wavelength $1.55\,\mu m$, and supports an HE mode with the propagation wavenumber $\beta_{\text{HE}} = 5.8912\,\mu m^{-1}$. The periodicity Λ of the FBG is chosen to satisfy the Bragg condition $\pi/\Lambda = \beta_{\text{HE}}$

(a)

(b)
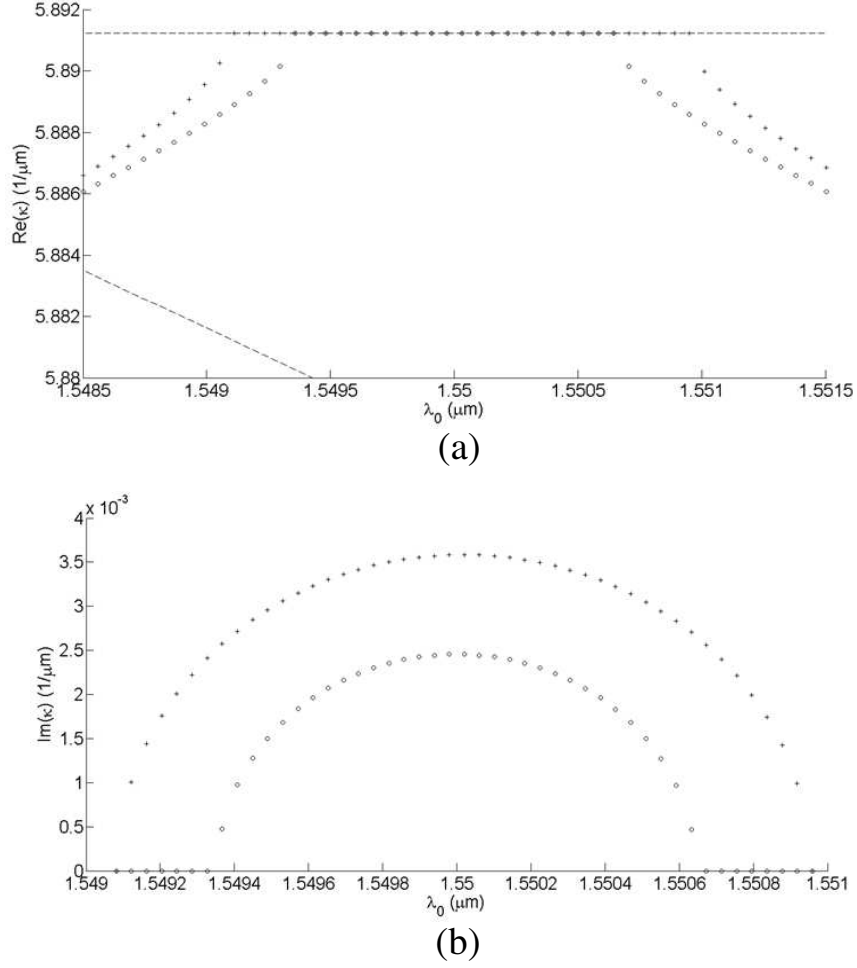
Figure 2. (a) The real and (b) imaginary parts of the Bloch wavenumber of the *bounded* Bloch eigenmode of the first structure in Section 4, extracted by the proposed rigorous method (crosses) and CMT (circles). The dashed lines in part (a) depict π/Λ and $k_0\sqrt{\varepsilon_s}$.

at the vacuum wavelength $1.55\,\mu$m, and thus to ideally provide the prerequisite for Eqs. (21) and (22) of the CMT approach. Figs. 2(a) and 2(b) show the real and imaginary parts of the Bloch wavenumber extracted by the rigorous method, and by CMT, for this FBG.

For the second structure, $D = 8.55\,\mu$m. Therefore, the associated *unperturbed* fiber is multimode at the vacuum wavelength $1.55\,\mu$m, and supports a TE mode with the propagation wavenumber $\beta_{\mathrm{TE}} = 5.8779\,\mu$m^{-1}. The periodicity Λ of the FBG is chosen to satisfy the Bragg condition $\pi/\Lambda = \beta_{\mathrm{TE}}$ at the vacuum wavelength $1.55\,\mu$m. Figs. 3(a) and 3(b) depict the results for this case.

For each of the above-mentioned structures, the real and imaginary parts of the Bloch wavenumber extracted by the proposed rigorous method converge with only $M = 1$, i.e., with $N = 3$ and $N = 2$ for the real and imaginary parts respectively.

The value of δ is 0.0064, yet the percent error of CMT in extraction of the imaginary part of the Bloch wavenumber is between 30 and 100 for the first example, and between 60 and 100 for the second example. However small δ is taken, the percent error of CMT is large, especially for the imaginary part of the Bloch wavenumber.

This error is probably due to the facts that; first, c_{β_0} (or $c_{-\beta_0}$) in Eqs. (21) and (22) is assumed to be the coefficient of all the four transverse components of the electromagnetic fields of the forward (or backward) bounded mode of the *unperturbed* fiber in the CMT expansions; and second, the radiation
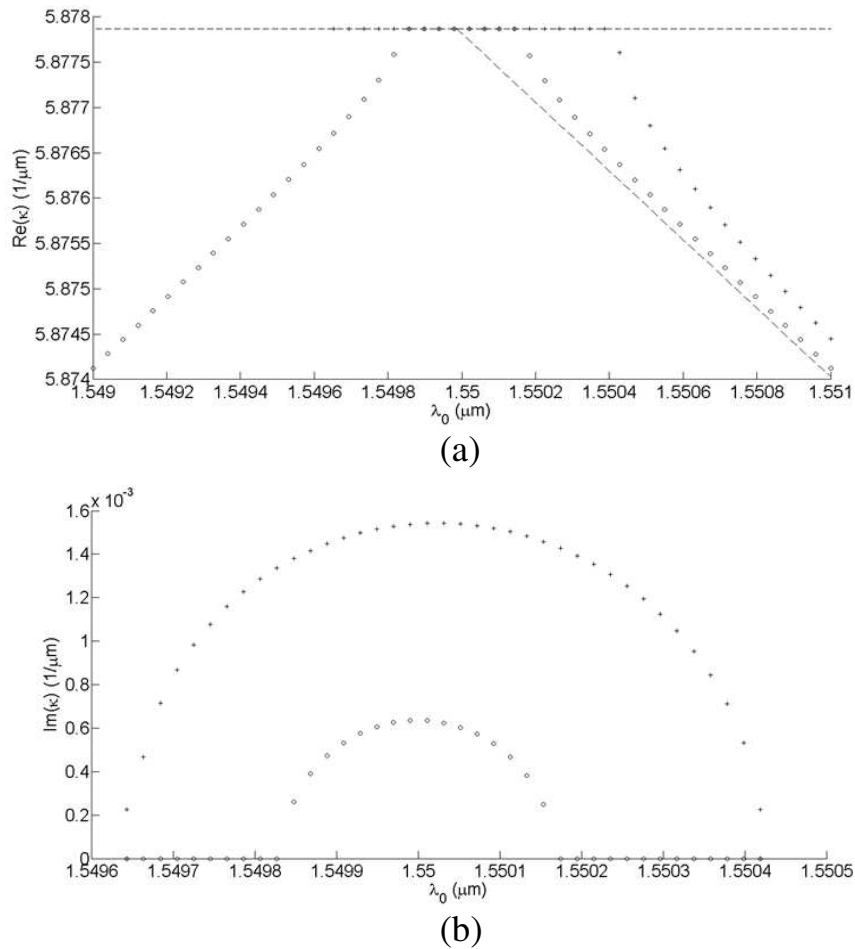
Figure 3. (a) The real and (b) imaginary parts of the Bloch wavenumber of the *bounded* Bloch eigenmode of the second structure in Section 4, extracted by the proposed rigorous method (crosses) and CMT (circles). The dashed lines in part (a) depict π/Λ and $k_0\sqrt{\varepsilon_s}$. For vacuum wavelengths shorter than $1.5496\,\mu$m, the bounded Bloch eigenmode no longer exists.

modes of the *unperturbed* fiber are excluded from the CMT expansions.

If an FBG with a periodicity Λ is excited by a forward bounded mode of its associated *unperturbed* fiber with a propagation wavenumber $\beta_0 \approx \pi/\Lambda$, this mode and its backward version (with the propagation wavenumber $-\beta_0$) have the most contribution in the CMT expansions, whereas each of the radiation modes of the *unperturbed* fiber only has an *infinitesimal* contribution, and is excluded from the CMT expansions, hence Eqs. (21) and (22). Nonetheless, the fact that there is a *continuum* of the radiation modes of the *unperturbed* fiber, which are all excluded from the CMT expansions, can potentially manifest itself in the inaccuracy of the resultant Bloch eigenmode. Even assuming that CMT accurately predicts the percentages of the reflected and transmitted powers, it is not a convincing argument for the accuracy of the Bloch eigenmodes obtained by CMT. As a simpler case in a different context, it is evident that all the incident power is reflected from a short-circuit load in a lossless transmission line irrespective of the wavenumber of the eigenmode supported by the transmission line.

The importance of the proposed rigorous method is even more considerable when modulation depth of refractive index is increased and/or when the accurate Bloch eigenmode of a fiber grating in the linear regime is to be used in a nonlinear analysis of the same structure via perturbation methods.

APPENDIX A.

Maxwell's curl equations read:

$$\nabla_t \times (\hat{z} E_z) + \hat{z} \times \frac{\partial}{\partial z} \vec{E}_t = -j\omega \vec{B}_t, \tag{A1}$$

$$\nabla_t \times \vec{E}_t = -j\omega \hat{z} B_z, \tag{A2}$$

$$\nabla_t \times (\hat{z} H_z) + \hat{z} \times \frac{\partial}{\partial z} \vec{H}_t = j\omega \vec{D}_t, \tag{A3}$$

and

$$\nabla_t \times \vec{H}_t = j\omega \hat{z} D_z. \tag{A4}$$

The discussion is limited to a material which is linear and isotropic with a relative permittivity ε_r and a relative permeability μ_r. Therefore, Eq. (A1) states that:

$$\vec{H}_t = \frac{1}{j\omega\mu_0\mu_r} \left[\hat{z} \times \nabla_t E_z - \frac{\partial}{\partial z} \hat{z} \times \vec{E}_t \right]. \tag{A5}$$

From Eqs. (A3) and (A5) it is evident that:

$$\vec{H}_t = \frac{1}{j\omega\mu_0\mu_r} \left[\hat{z} \times \nabla_t E_z - \frac{1}{j\omega\varepsilon_0} \frac{\partial}{\partial z} \left[\frac{1}{\varepsilon_r} \left[\nabla_t H_z - \frac{\partial \vec{H}_t}{\partial z} \right] \right] \right],$$

and therefore:

$$k_0^2 \mu_r \vec{H}_t + \frac{\partial}{\partial z} \left(\frac{1}{\varepsilon_r} \frac{\partial \vec{H}_t}{\partial z} \right) = -j\omega\varepsilon_0 \hat{z} \times \nabla_t E_z + \frac{\partial}{\partial z} \left(\frac{1}{\varepsilon_r} \nabla_t H_z \right). \tag{A6}$$

Assuming that ε_r and μ_r depend only on the longitudinal coordinate z, and using both of Eq. (A4) and the transverse curl $(\nabla_t \times)$ of Eq. (A6), the following relationship is obtained:

$$\nabla_t^2 E_z + \frac{\partial}{\partial z} \left(\frac{1}{\varepsilon_r} \frac{\partial (\varepsilon_r E_z)}{\partial z} \right) + k_0^2 \mu_r \varepsilon_r E_z = 0, \tag{A7}$$

which is the same as Eq. (7) when $\mu_r = 1$.

Along the same line, Eq. (8) is derived from Eqs. (A3), (A1), and (A2).

REFERENCES

1. Passaro, V., R. Diana, and M. N. Armenise, "Optical fiber Bragg gratings. Part I. Modeling of infinitely long gratings," *JOSA A*, Vol. 19, No. 9, 1844–1854, 2002.
2. Lalanne, P. and E. Silberstein, "Fourier-modal methods applied to waveguide computational problems," *Opt. Lett.*, Vol. 25, No. 15, 1092–1094, 2000.
3. Silberstein, E., P. Lalanne, J. P. Hugonin, and Q. Cao, "Use of grating theories in integrated optics," *JOSA A*, Vol. 18, No. 11, 2865–2875, 2001.
4. Lu, Y. C., L. Yang, W. P. Huang, and S. S. Jian, "Unified approach for coupling to cladding and radiation modes in fiber Bragg and long-period gratings," *IEEE J. Lightw. Techn.*, Vol. 27, No. 11, 1461–1468, 2009.
5. Song, N., J. Mu, and W. P. Huang, "Application of the complex coupled-mode theory to optical fiber grating structures," *IEEE J. Lightw. Techn.*, Vol. 28, No. 5, 761–767, 2010.
6. Li, L., "Note on the *S*-matrix propagation algorithm," *JOSA A*, Vol. 20, No. 4, 655–660, 2003.
7. Moharam, M. G. and T. K. Gaylord, "Three-dimensional vector coupled-wave analysis of planar-grating diffraction," *JOSA*, Vol. 73, No. 9, 1105–1112, 1983.
8. Szkopek, T., V. Pasupathy, J. E. Sipe, and P. W. E. Smith, "Novel multimode fiber for narrow-band Bragg gratings," *IEEE J. Sel. Top. Quant. Electr.*, Vol. 7, No. 3, 425–433, 2001.

9. Mohammed, W., X. Gu, and P. W. E. Smith, "Full vectorial modal analysis of specialty fibers and their Bragg grating characterization," *Appl. Opt.*, Vol. 45, No. 14, 3307–3316, 2006.

10. Erdogan, T. and J. E. Sipe, "Tilted fiber phase gratings," *JOSA A*, Vol. 13, No. 2, 296–313, 1996.

11. Erdogan, T., "Fiber grating spectra," *IEEE J. Lightw. Techn.*, Vol. 15, No. 8, 1277–1294, 1997.

12. Erdogan, T., "Cladding-mode resonances in short- and long-period fiber grating filters," *JOSA A*, Vol. 14, No. 8, 1760–1773, 1997.

13. Lu, C. and Y. Cui, "Fiber Bragg grating spectra in multimode optical fibers," *IEEE J. Lightw. Techn.*, Vol. 24, No. 1, 598–604, 2006.

14. Yariv, A. and P. Yeh, *Photonics: Optical Electronics in Modern Communication*, Oxford, New York, 2007.

15. Li, L., "Use of Fourier series in the analysis of discontinuous periodic structures," *JOSA A*, Vol. 13, No. 9, 1870–1876, 1996.

16. Nishihara, H., M. Haruna, and T. Suhara, *Optical Integrated Circuits*, McGraw-Hill, New York, 1989.